Simulation and optimisation of a two-stage/two-pass reverse osmosis system for improved removal of chlorophenol from wastewater

M. A. Al-Obaidi [1, 2], C. Kara-Zaïtri [1] and I. M. Mujtaba [1, *]

[1] Chemical Engineering, School of Engineering, Faculty of Engineering and Informatics. University of Bradford. Bradford, West Yorkshire BD7 1DP, UK
[2] Middle Technical University, Iraq – Baghdad
***Corresponding author, Tel.: +44 (0) 1274 233645**
E-mail address: I.M.Mujtaba@bradford.ac.uk

Abstract

Reverse osmosis (RO) has become a common method for treating wastewater and removing several harmful organic compounds because of its relative ease of use and reduced costs. Chlorophenol is a toxic compound for humans and can readily be found in the wastewater of a wide range of industries. Previous research in this area of work has already provided promising results in respect of the performance of an individual spiral wound RO process for removing chlorophenol from wastewater, but the associated removal rates have stayed stubbornly low. The literature has so far confirmed that the efficiency of eliminating chlorophenol from wastewater using a pilot-scale of an individual spiral wound RO process is around 83 %, compared to 97 % for dimethylphenol. This paper explores the potential of an alternative configuration of two-stage/two-pass RO process for improving such low chlorophenol rejection rates via simulation and optimisation. The operational optimisation carried out is enhanced by constraining the total recovery rate to a realistic value by varying the system operating parameters according to the allowable limits of the process. The results indicate that the proposed configuration has the potential to increase the rejection of chlorophenol by 12.4 % while achieving 40 % total water recovery at an energy consumption of 1.949 kWh/m^3.

Keywords: Modeling; Optimisation; Multi-stage Reverse Osmosis; Two-Stage/Two-Pass Design; Water Treatment; Chlorophenol Removal.

1. Introduction

Development of novel and diverse water treatment technologies are continuously evolving due to strict water quality regulations with emphasis on trace contaminants (Abdulgader et al., 2013). Effluents of many industrial applications contain a variety of micro-pollutants, which are

released into a variety of water resources. Such micro-pollutants not only disrupt the biological ecosystem, but they also pose real threat to public health. They include phenol and phenolic compounds, which are colorless (at room temperature) crystalline substances, consisting of hydroxyl and aromatic hydrocarbon group. They are highly toxic even in the small amounts that they can be in the effluents from various industries including refineries, and fertiliser, pesticide, chemical, petrochemical, wood, and paint industries (Kujawski *et al.*, 2004; Karigar *et al.*, 2006; Ahmed *et al.*, 2010). More importantly, the existence of a stable benzene ring in phenol and phenolic derivatives has increased their resistance to biological decomposition. Much recent research has focused on the removal of chlorophenol (suspected carcinogen), which is formed following the release of phenol into the environment (especially water). This is because it undergoes an active reaction with chlorine to form chlorophenol, which is more persistent than phenol and have a higher toxicity level (Irfanudeen *et al.*, 2015). The World Health Organization (WHO) and the U.S. Environmental Protection Agency (US EPA) have set the phenol concentration to 1 μg/l in drinking water (Hsieh *et al.*, 2008; Gami *et al.*, 2014). The Agency of Toxic Substances and Disease Registry (ATSDR) limited the concentration of dimethylphenol to a maximum of 0.05 ppm in surface water (ATSDR, 2015). Also, the Japan Environmental Governing Standards constrained phenol concentration to 5 mg/l in water sources (JEGS, 2016).

To resolve this problem, there has been several attempts to degrade the phenol and phenolic compounds from water using different treatment methods such as distillation processes, activated carbon adsorption, ion exchange, solvent extraction, chlorine dioxide, ozonation, UV/H_2O_2, catalyst wet air oxidation, biological methods, and membrane technology (Abdulgader *et al.*, 2013; Jain *et al.*, 2004; Busca *et al.*, 2008). Interestingly, the UV/H_2O_2 is considered as the most used technology for achieving the restricted limits of phenol required. However, this technology not only consumes a lot of energy, but it also potentially increases the carbon concentration in re-used water (Fujioka *et al.*, 2014a). However, due to continuous improvement in design and fabrication of membranes (Ng *et al.*, 2013; Lalia *et al.*, 2013), amongst all these treatment processes, the RO process (energy saving process) are being widely used for removing organic compounds, such as sulphate, copper, cadmium, nickel, chromium, and phosphate, from water with very high efficiency of around 99% (Mohammadi *et al.*, 2009; Madaeni and Koocheki, 2010; Urgun-Demirtas *et al.*, 2012; Doederer *et al.*, 2014; Bunani *et al.*, 2015). The efficiency of the RO process for removing organic compounds from water is highly dependent on the nature

of the compound and molecular weight, the operating conditions, the pH of the feed (which controls the extent of organic dissociation in the solution), the matrix of the membrane and the solute-membrane polymer interaction. All these parameters affect the sorption of organic compounds through the membrane body. More importantly, the laboratory investigation of Sundaramoorthy *et al.* (2011) confirms that the efficiency of eliminating chlorophenol from water using a pilot-scale of an individual spiral wound RO process is around 83%, compared to 97% for dimethylphenol (Srinivasan *et al.*, 2011). The 83 % chlorophenol rejection rate is obtained using 13.58 atm, 2.583×10^{-4} m^3/s and 31 °C of operating feed pressure, flow rate and temperature respectively, with 22 % total water recovery at an energy consumption of 2.034 kWh/m^3. The relatively low chlorophenol rejection rate is probably attributed to its high hydrophobicity properties in water (easily dissolved in water) in addition to its high activity due to the presence of hydroxyl group, which makes it easily penetrable through the membrane. Existing literature shows that the experimental study of Sundaramoorthy *et al.* (2011) is the only study that deals with the removal of chlorophenol from water using the spiral wound module of RO process but with only one membrane RO module.

This paper explores the feasibility of an alternative RO process configuration of two-stage/two-pass RO process instead of a single stage considered by Sundaramoorthy *et al.* (2011) for improving the current low chlorophenol rejection via simulation and optimisation. The work of Hafez and E1-Manharawy (2004) motivated this work who used a full-scale plant using several technologies such as pH-adjustment, addition of the polymer coagulant, chlorination, dechlorination, filtration including RO membrane separation of two-stage/two-pass design of medium pressure RO membrane (maximum 16 bar) process to remove chromium from tannery effluent. The results showed that the plant can remove 99.9 % of chromium based on the combined technologies used.

2. Multi-stage RO process model

The successful lumped and distributed modelling of an individual spiral wound RO process for the removal of phenol and its derivatives from water has been achieved by Srinivasan *et al*, (2009), Sundaramoorthy *et al.* (2011), Srinivasan *et al.* (2010), Srinivasan *et al.* (2011), Al-Obaidi and Mujtaba (2016), Al-Obaidi *et al.* (2017a), Al-Obaidi *et al.* (2017b), Al-Obaidi *et al.* (2017c) and Al-Obaidi *et al.* (2017d). Nevertheless, the efficiency of the two-stage/two-pass

design of multi-stage RO system considering the chlorophenol removal from wastewater has not been investigated yet. Therefore, this research elucidates the capacity of this design with implementing simulation and optimisation studies to maximise the rejection parameter at an official total recovery rate of 40% and acceptable limit of energy consumption. Recently, Al-Obaidi *et al.* (2017e) developed a specific steady state model based on the solution-diffusion model, which showed an acceptable agreement with experimental data of dimethylphenol removal from water. This same model will be calibrated for use in the two-stage/two-pass multi-stage RO process for the removal of chlorophenol. All model equations are presented in Table A.1 of Appendix A, while Tables A.2 and A.3 show the degree of freedom analysis of the model for the convenience of the readers. The intended outcome of this research is to achieve a better RO network for removing chlorophenol from water than those used in the past. gPROMS Model Builder 4.0 (Process System Enterprise Ltd., 2001) is used in this work for simulation and optimisation.

3. Description of the two-stage/two-pass RO process

Fig. 1 shows a schematic diagram of the proposed full-scale two-stage/two-pass design RO process to treat water containing chlorophenol. The multi-stage RO process contains 7 pressure vessels connected in three stages, where each pressure vessel holds only one spiral wound module of a commercial thin film composite membrane element type (Ion Exchange, India). The membrane selected is identical to the one used by Sundaramoorthy *et al.* (2011) to investigate the performance of an individual membrane RO process for chlorophenol removal from its aqueous solutions of different concentrations. Therefore, the membrane transport parameters of water A_w and chlorophenol B_s and membrane friction factor b are assumed to be the same as what investigated by Sundaramoorthy *et al.* (2011). The specifications of the selected membrane are given in Table 1. The first and second stages come with a series configuration of 3:2 pressure vessels where the water is directly fed to the first stage of three parallel pressure vessels and then the blended high concentration stream is forwarded to the second stage of two parallel pressure vessels for further concentration. The combined low concentration permeate streams of the first and second stages are forwarded to the third stage for further processing in two parallel pressure vessels. Specifically, there are two high-pressure pumps at the entrance of the first and third stages, while a booster pump is connected to compensate the pressure drop of the first stage to

keep the identical feed plant pressure at the second stage. The two pumps deliver a maximum of 20 atm, i.e. the same values used by Sundaramoorthy *et al.* (2011). The augmentation of the two permeate streams of the first and second stages has the advantage of keeping the product of the third stage at low concentration. While, the concentrated two streams of the second and third stages are blended to form the outlet plant disposed stream.

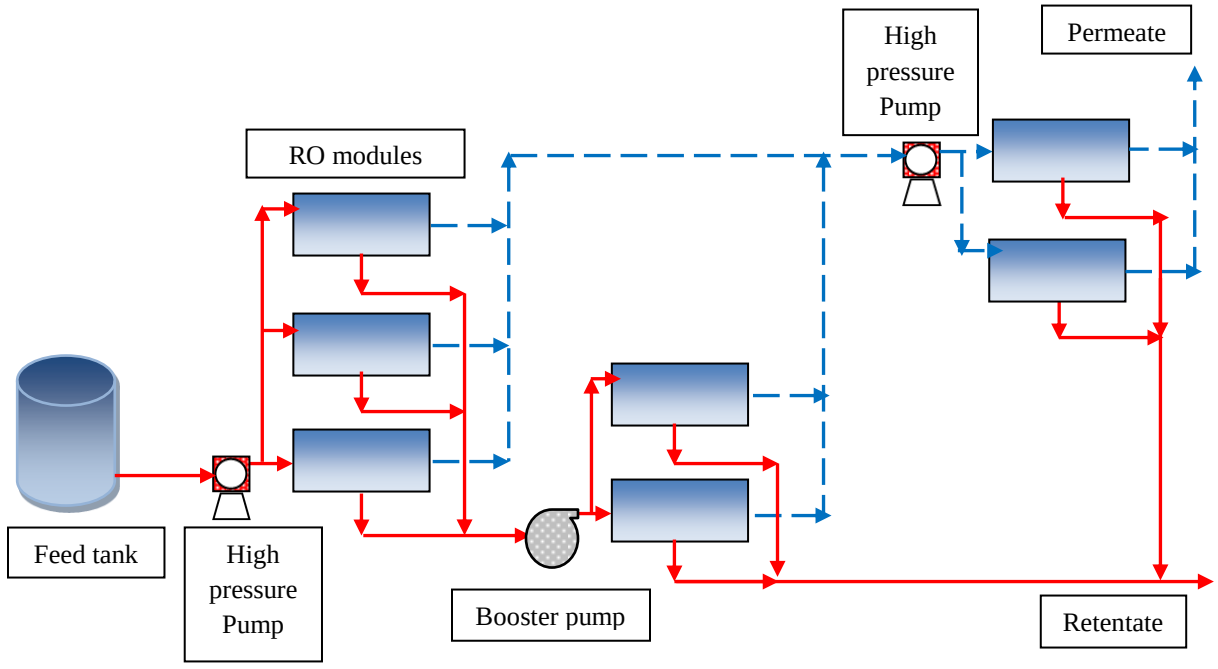

Fig. 1. Schematic diagram of the proposed two-stage/two-pass RO process

Table 1. The specification of Ion Exchange, India membrane module with the model parameters

Parameter	Value
Module configuration	Spiral wound
Membrane material	TFC Polyamide
Number of turns	30
Permeate channel thickness (t_p)	0.5 mm
Feed spacer thickness (t_f)	0.8 mm
Module diameter	0.0825 m
Module length (L)	0.934 m
Module width (W)	8.4 m
b	8529.45 $\left(\frac{atm\ s}{m^4}\right)$
A_w	9.5188x10^{-7} $\left(\frac{m}{atm\ s}\right)$
B_s	8.468x10^{-8} $\left(\frac{m}{s}\right)$
Molecular weight of chlorophenol	128.6 (gm/mol)

4. Simulation of the two-stage/two-pass RO process

Before optimisation of the process is considered a detailed simulation of the process is carried out to facilitate deeper insight of the impact of different operating conditions on the performance of the process. The simulation is carried out with chlorophenol concentration $C_{f(plant)}$ of 6.226x10^{-3} kmol/m³, which is equivalent to 800.66 ppm. Four cases were studied with different operating conditions of the plant feed flow rate $Q_{f(plant)}$, feed pressure $P_{f(plant)}$ and temperature $T_{(plant)}$ as shown below:

- 1.50x10^{-3} m³/s, 18 atm and 33 °C
- 7.749x10^{-4} m³/s, 15 atm and 32 °C
- 6.498x10^{-4} m³/s, 13 atm and 31 °C
- 5.40x10^{-4} m³/s, 12 atm and 30 °C

These operating conditions shown above are within the upper and lower limits of the manufacturer's membrane specification (given in Table 2 for each membrane module) to ensure the safe working of the process. Note, the simulation is carried out within temperature range of 30 to 33° C as considered by Sundaramoorthy *et al.* (2011), although the maximum allowed temperature is 40 °C. This is due to the fact that the temperature has significant impact on the model transport parameters (A_w and B_s) at higher temperatures (say 40 °C).

Table 2. The limits of operation of the spiral wound membrane element (Ion Exchange, India)

Parameter	Value
Maximum feed flow rate (m^3/s)	$1.0x10^{-3}$
Minimum feed flow rate (m^3/s)	$1.0x10^{-4}$
Maximum operating temperature T (°C) *	40
Maximum operating pressure (atm)	24
Maximum pressure drop (atm)	1.38

* Sundaramoorthy *et al.* (2011)

The simulation results of this process are given in Table 3. This shows a noticeable increase in chlorophenol rejection despite low recovery rate and variable energy consumption. The low recovery rate can be attributed to the use of arbitrary values (non-optimised values) of feed flow rate, operating pressure, and temperature. Having said this, Table 3 shows that the simultaneous reduction of the operating feed flowrate, pressure, and temperature can support the water recovery rate despite lower product flow rate and rejection parameter. This can be attributed to increased rate of concentration polarisation as a result to the increase of the residence time of the fluid inside the module, which occurred due to reduced operating feed flow rate. The net effect of this is a reduction of the permeate flow rate and an increase in the quantity of phenol penetrating the membrane, which finally retards the rejection parameter (Table 3). The results shown in Table 3 essentially highlight the advantages of the proposed configuration for the removal of chlorophenol. The next section will deal with the process optimisation to achieve a higher rejection rate while maintaining higher recovery rate but with an acceptable energy consumption.

Table 3. The simulation results of the two-stage/two-pass RO process at initial chlorophenol concentration of 6.226×10^{-3} kmol/m³

Simulation case	Total permeate concentration, kmol/m³	Product flow rate, m³/s	Total retentate concentration, kmol/m³	Retentate flow rate, m³/s	%Rejection (-)	%Recovery rate (-)	Energy consumption, kWh/m³
1	2.154×10^{-4}	2.326×10^{-4}	7.329×10^{-3}	1.267×10^{-3}	96.539	15.512	5.712
2	3.389×10^{-4}	1.798×10^{-4}	8.005×10^{-3}	5.950×10^{-4}	94.556	23.208	3.349
3	4.508×10^{-4}	1.454×10^{-4}	7.890×10^{-3}	5.043×10^{-4}	92.759	22.376	2.970
4	5.865×10^{-4}	1.248×10^{-4}	7.922×10^{-3}	4.151×10^{-4}	90.578	23.125	2.658

5. Optimisation of the two-stage/two-pass RO process

The optimisation process is based on maximising the chlorophenol rejection $Rej_{(Total)}$ (objective function) within the manufacturer's specification of membrane module (shown in Table 2). This includes the upper and lower limits of plant flow rate $Q_{f(plant)}$ and pressure drop per each module. However, the range of 30 to 33 °C and 5 atm to 20 atm as the operating temperature $T_{(plant)}$ and plant feed pressure $P_{f(plant)}$ respectively were selected to be within the transport parameters investigated and in line with the capacity of the pump used in the experimental work of Sundaramoorthy *et al.* (2011). Therefore, the optimisation methodology rightly manages the manipulation of the plant operating conditions in such a way that the determined limits of this configuration are not exceeded. Also, the optimisation considers the number of pressure vessels at the first stage as well as the promising total water recovery of 40 % at maximum chlorophenol rejection. A restricted constrain range of 1 to 2 kWh/m³ of total energy consumption $E_{(Total)}$ is held to secure the required low total energy consumption compared with the simulation results of Table 3. Finally, the overall pressure drop per each membrane module ΔP_{drop} is restricted at a maximum value of equal or less than the allowed value of 1.38 atm.

The optimisation problem can be mathematically written as presented in Table 4.

Table 4. The optimisation problem explained

Max $Rej_{(Total)}$ $Q_{f(plant)}, P_{f(plant)}, T_{(plant)}$
Subject to: Equality constraints: Process Model: $f(x, u, v) = 0$
Inequality constraints of the plant: Inlet pressure: (5 atm) $P_{f(plant)}{}^{L} \leq P_{f(plant)} \leq P_{f(plant)}{}^{U}$ (20 atm)
Inlet feed flow rate: ($3x10^{-4}$ m³/s) $Q_{f(plant)}{}^{L} \leq Q_{f(plant)} \leq Q_{f(plant)}{}^{U}$ ($3x10^{-3}$ m³/s)
Operating temperature: (30 °C) $T_{(plant)}{}^{L} \leq T_{(plant)} \leq T_{(plant)}{}^{U}$ (33 °C)
Inequality constraints of the element: Inlet pressure: (5 atm) $P_{f(in)}{}^{L} \leq P_{f(in)} \leq P_{f(in)}{}^{U}$ (20 atm)
Inlet feed flow rate: ($1.0x10^{-4}$ m³/s) $Q_{f}{}^{L} \leq Q_{f} \leq Q_{f}{}^{U}$ ($1.0x10^{-3}$ m³/s)
Operating temperature: (30 °C) $T^{L} \leq T \leq T^{U}$ (33 °C)
Pressure drop per each element: $\Delta P_{drop} \leq 1.38$
Limits of total energy consumption: 1 kWh/m³ $\leq E_{(Total)} \leq$ 2 kWh/m³

The nonlinear algebraic equations of the model used in this work can be written in a compact form $f(x, u, v) = 0$, where x is the set of all algebraic variables, u is the set of decision variables need to be optimised and v represents the constant parameters of the model. The function f is assumed to be continuously differentiable with respect to all their arguments. The optimization problem was solved using the SQP method of the gPROMS software suit.

6. Optimisation results

Table 5 shows the optimisation results of chlorophenol rejection, total water recovery and total energy consumption and provides the optimised operating parameters of feed pressure, feed flow rate and operating temperature of three optimisation cases. The results of case 1 confirm the ability of the proposed configuration to elevate the chlorophenol experimental rejection of Sundaramoorthy *et al.* (2011) by about 12.4 % (from 83 % to 93.325 %) with 81 % increase in total water recovery (from 22 % to 40 %), with a reduction in total energy consumption of about 4 % (from 2.034 to 1.95 kWh/m³). In general, the optimised parameter values have a positive impact on the total energy consumption compared to simulation results shown in Table 3. The allowed constraint of total energy consumption is increased to the range of 2 to 3 kWh/m³ in cases 2 and 3 to investigate the process performance at higher energy consumption. Table 5 shows that higher process energy consumption to 2.50 and 2.874 kWh/m³ due to higher pressure and higher pumping requirement has insignificant impact on chlorophenol rejection. Therefore, case 1 yields the best optimisation results.

Table 5. The optimisation results of two-stage/two-pass RO process at inlet chlorophenol concentration of 6.226E-3 kmol/m³

	The operating conditions			The optimised parameters		
Case	Pressure, $P_{f(plant)}$ atm	Flow rate, $Q_{f(plant)}$ m³/s	Temperature, $T_{(plant)}$ °C	%Rejection, $Rej_{(Total)}$	%Recovery, $Rec_{(Total)}$	Energy consumption, $E_{(Total)}$ kWh/m³
1	13.245	3.890×10^{-4}	33.0	93.325	40.001	1.949
2	16.860	5.176×10^{-4}	33.0	94.487	40.000	2.500
3	19.307	6.049×10^{-4}	33.0	95.019	40.000	2.874

The optimisation results shown above clearly confirm the merits of using a two stage/two pass RO network, which yield a higher chlorophenol removal rate from wastewater, and at a reasonable water recovery level and energy consumption. This is despite the fact that chlorophenol has high hydrophobicity properties in water**.**

7. Conclusions

Although a two-stage/two-pass RO configuration has already been used for the removal of chromium from wastewater, the same has never been tested for the removal of chlorophenol. This study, based on simulation and optimisation, has demonstrated that a two-stage/two-pass RO configuration yields improved results for the removal of chlorophenol from wastewater in comparison to previous attempts. The simulation results indicate a noticeably higher rejection of chlorophenol as one of the high toxic compounds found in water. The requirements of reducing the total energy consumption and at the same time elevating the rejection parameter has been achieved using an optimisation study manipulating the process parameters within allowed operational limits. A maximum of 93.3 % chlorophenol rejection has been obtained for the proposed configuration 12.4 % higher than the latest published work. The results also show that a significantly higher recovery rate of 40 % at a lower energy consumption of 1.949 kWh/m³ is possible to the proposed RO network.

Nomenclature

A : Effective area of the membrane (m²)

A_w : Solvent transport coefficient (m/atm s)

b : Feed and permeate channels friction parameter (atm s/m^4)

B_s : Solute transport coefficient (m/s)

C_b : The bulk feed solute concentrations at the feed channel (kmol/m³)

C_f : The inlet feed solute concentrations at the feed channel (kmol/m³)

$C_{f(plant)}$: The inlet chlorophenol concentration of the plant (kmol/m³)

C_m : The dimensionless solute concentration in Eq. (5) (dimensionless)

C_p : The permeate solute concentration at the permeate channel (kmol/m³)

C_w : The solute concentration on the membrane surface at the feed channel (kmol/m³)

D_b : The solute diffusion coefficient of feed at the feed channel (m²/s)

D_p : The solute diffusion coefficient of feed at the permeate channel (m²/s)

de_b : The equivalent diameters of the feed channel (m)

de_p : The equivalent diameters of the permeate channel (m)

E : The specific energy consumption of high pressure pump of each module (kW h/m³)

$E_{(Total)}$: Total energy consumption of the plant (kW h/m³)

J_s : The solute molar flux through the membrane (kmol/m² s)

J_w : The permeate flux (m/s)

k : The mass transfer coefficient at the feed channel (m/s)

L : The length of the membrane (m)

m_f : Parameter in Eqs. (10) and (11)

$P_{f(in)}$: The inlet feed pressure (atm)

$P_{f(out)}$: The outlet feed pressure (atm)

$P_{f(plant)}$: Plant feed pressure (atm)

P_p : The permeate channel pressure (atm)

Q_b : The bulk feed flow rate at the feed channel (m³/s)

Q_f : The inlet feed flow rate at the feed channel (m³/s)

$Q_{f(plant)}$: Plant feed flow rate (m³/s)

Q_p : The permeate flow rate at the permeate channel (m³/s)

Q_r : The retentate flow rate at the feed channel (m³/s)

R : The gas low constant (R = 0.082 atm m³/ K kmol)

Re_b : The Reynold number at the feed channel (dimensionless)

Rec : Total permeate recovery (dimensionless)

$Rec_{(Total)}$: Total water recovery rate of the plant (dimensionless)

Rej : The solute rejection coefficient (dimensionless)

$Rej_{(Total)}$: Total chlorophenol rejection of the plant (dimensionless)

Re_p : The Reynold number at the permeate channel (dimensionless)

T : The feed temperature (°C)

$T_{(plant)}$: Plant feed temperature (°C)

t_f : Height of feed channel (m)

t_p : Height of permeate channel (m)

U_b : The bulk feed velocity at the feed channel (m/s)

W : The membrane width (m)

Subscript

μ_b : The Feed viscosity at the feed channel (kg/m s)

μ_p : The permeate viscosity at the permeate channel (kg/m s)

ρ_b : The feed density at the feed channel (kg/m³)

ρ_p : The permeate density at the permeate channel (kg/m³)

ρ_w : Molal density of water (55.56 kmol/m³)

θ : Parameter in Eq. (24)

ΔP_{drop} : The pressure drop per each element (atm)

References

Abdulgader, H.A., Kochkodan, V. Hilal, N. 2013. Hybrid ion exchange – Pressure driven membrane processes in water treatment: A review. Separation and Purification Technology, 116, 253–264

Agency for toxic substances and disease registry (ATSDR), division of toxicology and human health sciences, 2015. Substance Priority List. https://www.atsdr.cdc.gov/spl/index.html

Ahmed S., Rasul M. G., Martens W. N., Brown R. and Hashib M. A., 2010. Heterogeneous photocatalytic degradation of phenols in wastewater: A review on current status and developments, *Desalination*, 261, 3-18.

Al-Obaidi M. A., and Mujtaba I. M., 2016. Steady state and dynamic modeling of spiral wound waste water reverse osmosis process. *Computers and Chemical Engineering*, 90, 278-299.

Al-Obaidi M. A., Li J- P., Kara-Zaïtri C., and Mujtaba I. M., 2017a. Optimisation of reverse osmosis based wastewater treatment system for the removal of chlorophenol using genetic algorithms. *Chemical Engineering Journal*, 316, 91-100.

Al-Obaidi M. A., Kara-Zaïtri C., and Mujtaba I. M., 2017b. Wastewater treatment by spiral wound reverse osmosis: Development and validation of a two dimensional process model. *Journal of Cleaner Production*, 140, 1429-1443.

Al-Obaidi M. A., Kara-Zaitri C., and Mujtaba I. M., 2017c. Modeling of a spiral-wound reverse osmosis process and parameter estimation. *Desalination and Water Treatment,* 69, 93-101.

Al-Obaidi M. A., Kara-Zaitri C., and Mujtaba I. M., 2017d. Removal of phenol from wastewater using spiral-wound reverse osmosis process: model development based on experiment and simulation. Accepted in *Journal of Water Process Engineering* (in press).

Al-Obaidi M. A., Kara-Zaïtri C., and Mujtaba I. M., 2017e. Optimisation of membrane design parameters of a spiral-wound reverse osmosis module for high rejection of dimethylphenol from wastewater at low energy consumption. Proceedings of the 27th European Symposium on Computer Aided Process Engineering – ESCAPE 27, October 1st - 5th, 2017, Barcelona, Spain.

Bunani S., Yörükoğlu E., Yüksel Ü., Kabay N., Yüksel M., Sert G., 2015. Application of reverse osmosis for reuse of secondary treated urban wastewater in agricultural irrigation. *Desalination,* 364, 68-74.

Doederer K., Farré M. J., Pidou M., Weinberg H. S., Gernjak W., 2014. Rejection of disinfection by-products by RO and NF membranes: Influence of solute properties and operational parameters. *Journal of Membrane Science*, 467, 195-205.

Fujioka T. 2014a. *Assessment and optimisation of N-nitrosamine rejection by reverse osmosis for planned potable water recycling applications*. Ph.D. Theses, University of Wollongong.

Fujioka T., Khan S. J., Mcdonald J. A., Roux A., Poussade Y., Drewes J. E., and Nghiem L. D., 2014b. Modelling the rejection of N-nitrosamines by a spiral-wound reverse osmosis system: Mathematical model development and validation. *Journal of Membrane Science*, 454, 212-219.

Gami A. A., Shukor M. Y., Abdul Khalil K., Dahalan F. A., Khalid A. and Ahmad S. A., 2014. Phenol and its toxicity. *Journal of Environmental Microbiology and Toxicology*, 2(1), 11-24.

Hafez A., and E1-Manharawy S., 2004. Design and performance of the two-stage/two-pass RO membrane system for chromium removal from tannery wastewater. Part 3. *Desalination,* 165, 141-151.

Hsieh F. M., Huang C., Lin T. F., Chen Y. M., and Lin J. C., 2008. Study of sodium tripolyphosphate-crosslinked chitosan beads entrapped with Pseudomonas putida for phenol degradation. *Process Biochem*, 43, 83-92.

Irfanudeen N. M., Prakash I. A., Saundaryan R., Alagarraj K., Goel M., and Kumar K. R., 2015. The potential of using low cost naturally available biogenic substrates for biological removal of chlorophenol. *Bioresource Technology*, 196, 707-711.

Jain A. K., Gupta V. K., Jain S., and Suhas, 2004. Removal of chlorophenols using industrial wastes. *Environ. Sci. Technol*., 38, 1195-1200.

Japan Environmental Governing Standard (JEGS). Department of Defence. Chapter 4: Wastewater. Japan. Barron S. Headquarters, U.S. Forces Japan. 2016; 10, 57.

Karigar C., Mahesh A., Nagenahalli M., and Yun D. J., 2006. Phenol degradation by immobilized cells of Arthrobacter citreus. *Biodegradation*, 17, 47-55.

Koroneos C., Dompros A., and Roumbas G., 2007. Renewable energy driven desalination systems modelling. *J. Cleaner Prod.,* 15, 449-464.

Kujawski W., Warszawski A., Ratajczak W., Porębski T., Capała W., and Ostrowska I., 2004. Removal of phenol from wastewater by different separation techniques. *Desalination,* 163, 287-296.

Lalia, B.S., Kochkodan, V. Hashaikeh, R., Hilal, N. 2013. A review on membrane fabrication: Structure, properties and performance relationship. Desalination 326, 77–95

Madaeni S. S., and Koocheki S., 2010. Influence of di-hydrogen phosphate ion performance of polyamide reverse osmosis membrane for nitrate and nitrite removal. *J. Porous Mater*. 17, 163-168.

Mohammadi H., Cholami M., and Rahimi M., 2009. Application and optimization in chromium-contaminated wastewater treatment of the reverse osmosis technology. *Desalination and Water Treatment,* 9, 229-233.

Ng, L.W., Mohammad, A.W., Leo, C.P., Hilal, N., 2013. Polymeric membranes incorporated with metal/metal oxide nanoparticles: A comprehensive review. Desalination 308, 15–33.

Process System Enterprise Ltd., gPROMS Introductory User Guide. London: Process System Enterprise Ltd., 2001.

Srinivasan G., Sundaramoorthy S., and Murthy D. V. R., 2009. Separation of dimethyl phenol using a spiral-wound RO membrane– Experimental and parameter estimation studies. *Desalination*, 243, 170-181.

Srinivasan G., Sundaramoorthy S., and Murthy D. V. R., 2010. Spiral wound reverse osmosis membranes for the recovery of phenol compounds – Experimental and parameter estimation studies. *American Journal of Engineering and Applied Science*, 3(1), 31-36.

Srinivasan G., Sundaramoorthy S., and Murthy D. V. R., 2011. Validation of an analytical model for spiral wound reverse osmosis membrane module using experimental data on the removal of dimethylphenol. *Desalination*, 281, 199-208.

Sundaramoorthy S., Srinivasan G., and Murthy D. V. R., 2011. An analytical model for spiral wound reverse osmosis membrane modules: Part II — Experimental validation. *Desalination*, 277(1-3), 257-264.

Urgun-Demirtas M., Benda P. L., Gillenwater P. S., Negri M. C., Xiong H., Snyder S. W., 2012. Achieving very low mercury levels in refinery wastewater by membrane filtration. *Journal of Hazardous Materials*, 215– 216, 98-107.

Appendix A

Table A.1. The mathematical modelling of a spiral-wound RO system of Al-Obaidi *et al.* (2017e)

Model Equations	Specifications	Eq. no.
$J_w = A_w \left[\left(\frac{\left(P_{f(in)}+P_{f(out)}\right)}{2} - P_p\right) - \left(R\,(T+273.15)\,(C_w - C_p)\right)\right]$	The permeate flux (m/s)	1
$J_s = B_s\,(C_w - C_p)$	The solute flux (kmol/m² s)	2
$\frac{(C_w - C_p)}{(C_b - C_p)} = exp\left(\frac{J_w}{k}\right)$	The wall solute concentration (kmol/m³)	3
$k = \frac{147.4\,D_b\,Re_b^{0.13}\;Re_p^{0.739}\,C_m^{0.135}}{2\,t_f}$	The mass transfer coefficient (m/s) (Srinivasan *et al.*, 2011)	4
$C_m = \frac{C_b}{\rho_w}$	The dimensionless solute concentration (dimensionless)	5
$D_b = 6.725x10^{-6}\;exp\left\{0.154x10^{-3}\,(C_f\,x18.0125)\;-\frac{2513}{(T+273.15)}\right\}$	The diffusivity parameter at the feed channel (m²/s) (Koroneos, 2007)	6
$D_p = 6.725x10^{-6}\;exp\left\{0.154x10^{-3}(C_p\,x18.0125)\;-\frac{2513}{(T+273.15)}\right\}$	The diffusivity parameter at the permeate channel (m²/s)	7
$\mu_b = 1.234x10^{-6}\,exp\left\{0.0212\,(C_f\,x18.0153) + \frac{1965}{(T+273.15)}\right\}$	The dynamic viscosity (kg/m s) at the feed channel	8
$\mu_p = 1.234x10^{-6}\,exp\left\{0.0212\,(C_p\,x18.0153) + \frac{1965}{(T+273.15)}\right\}$	The dynamic viscosity (kg/m s) at the permeate channel	9
$\rho_b = 498.4\,m_f + \sqrt{\left[248400\,m_f^2 + 752.4\,m_f\,C_f\,x18.01253\right]}$	The feed density (kg/m³)	10
$\rho_p = 498.4\,m_f + \sqrt{\left[248400\,m_f^2 + 752.4\,m_f\,C_p\,x18.01253\right]}$	The permeate density (kg/m³)	11
$m_f = 1.0069 - 2.757x10^{-4}\,(T)$	Parameter in Eqs. (10) and (11)	12
$Re_b = \frac{\rho_b\;de_b\,Q_b}{t_f\,W\,\mu_b}$	The Reynolds number at the feed channel (dimensionless)	13
$Re_p = \frac{\rho_p\;de_p\;J_w}{\mu_p}$	The Reynolds number at the permeate channel (dimensionless)	14
$de_b = 2t_f \qquad de_p = 2t_p$	The equivalent diameters of the feed and permeate channels (m)	15
$U_b = \frac{Q_b}{W\,t_f}$	The bulk feed velocity (m/s)	16
$Q_b = \frac{Q_f + Q_r}{2}$	The bulk feed flow rate (m³/s)	17
$C_b = \frac{C_f + C_r}{2}$	The bulk concentration (kmol/m³)	18
$C_p = \frac{C_f\,B_s}{\left(\frac{J_w}{\exp(\frac{J_w}{k})} + B_s\right)}$	The permeate solute concentration (kmol/m³)	19
$Q_f = Q_r + Q_p$	The retentate flow rate (m³/s)	20
$Q_f\,C_f = Q_r\,C_r + Q_p\,C_p$	The retentate concentration (kmol/m³)	21
$Q_p = J_w\,A$	The total permeated flow rate (m³/s)	22

Table A.1. The mathematical modelling of a spiral-wound RO system of Al-Obaidi *et al.* (2017e) (continued)

Model Equations	Specifications	Eq. no.
$P_{f(out)}=\left\{P_{f(in)} - \left(b\ L\ Q_f\right)+\left(\mathrm{b\ W}\ \theta \quad \left(\frac{L^2}{2}\right)\left(\Delta \mathrm{P_{f(out)}}\right)\right)\text{-}\left[\mathrm{b^2\ W}\ \theta \quad \left(\frac{L^3}{6}\right) Q_f\right] - \left[b^2\ W\ \theta \quad \left(\frac{W\ \theta}{b}\right)^{0.5}\left(\frac{L^3}{6}\right)\left(\Delta P_{f(out)} - \Delta P_{f(in)}\right)\right]\right\}$	The retentate pressure (Al-Obaidi *et al.*, 2017a)	23
$\theta = \frac{A_W\ B_S}{B_S+R\ (T+273.15)\ A_W\ C_p}$	Parameter in Eq. (23)	24
$\Delta P_{f(in)} = P_{f(in)} - P_p$	The pressure difference at the inlet edge (atm)	25
$\Delta P_{f(out)} = P_{f(out)} - P_p$	The pressure difference at the outlet edge (atm)	26
$Rec = \frac{Q_p}{Q_f}\ x100$	The total permeate recovery (dimensionless)	27
$Rej = \frac{C_f - C_p}{C_f} x100$	The solute rejection (dimensionless) (Srinivasan *et al.*, 2011)	28
$E = \frac{\left(\left(P_{f(in)}\ x101325\right) Q_f\ \right)}{\frac{Q_p\ \varepsilon pump}{36x10^5}}$	The specific consumption energy of HPP (kWh/m³)	29

Table A.2. Specifications of variables

Items	Total
Variables: $\mathrm{J_w}, \mathrm{J_s}, \theta, \mathrm{P_p}, P_{f(in)}, P_{f(out)}, \Delta P_{f(in)}, \Delta P_{f(out)}, \mathrm{R}, \mathrm{T}, \mathrm{C_f}, \mathrm{C_w}, \mathrm{C_b}, \mathrm{C_r},$ $\mathrm{C_p}, \mathrm{Q_f}, Q_r, \mathrm{Q_p}, Q_b, \mathrm{k}, \mathrm{Rec}, \mathrm{Rej}, \mathrm{de_b}, \mathrm{de_p}, \mathrm{C_m}, \mathrm{D_b}, \mathrm{D_p}, \mu_{\mathrm{b}}, \mu_{\mathrm{p}}, \rho_{\mathrm{b}}, \rho_{\mathrm{p}}, \mathrm{m_f}, \mathrm{Re_b}, \mathrm{Re_p},$ $U_b, E, \mathrm{A_w}, \mathrm{B_s}, \mathrm{L}, \mathrm{W}, \rho_{\mathrm{w}}, \mathrm{b}, \mathrm{t_f}$	43

Table A.2 shows the specification of the model where the total number of variables is 43, while the number of equations is 29 as can be seen in Table A.1, so:
D.F. = Total number of variables – Total number of equations
D.F. = 43 – 29 = 14
The number of parameters is 14 given in Table A.3. Therefore, the execution of the model simulation is completed successfully.

Table A.3. Specifications of inlet operating conditions and constant parameters

Parameter	Value
$C_f, Q_f, P_{f(in)}, P_p, T$	The operating conditions of each simulation
Feed channel friction parameter (b)	8529.45 $\left(\frac{atm\ s}{m^4}\right)$
Solvent transport coefficient (A_w)	$9.5188x10^{-7}$ $\left(\frac{m}{atm\ s}\right)$
Solute transport coefficient (B_s) (Chlorophenol)	$8.468x10^{-8}$ $\left(\frac{m}{s}\right)$
Module length (L)	0.934 m
Module width (W)	8.4 m
Feed spacer thickness (t_f)	0.8 mm
Permeate channel thickness (t_p)	0.5 mm
Molal density of water (ρ_w)	5.56 kmol/m³
Gas law constant (R)	0.082 (atm m³/K kmol)